



NMR in Commensurate and Incommensurate Spin Density Waves

To cite this article: E. Barthel *et al* 1993 *EPL* **21** 87

View the [article online](#) for updates and enhancements.

Related content

- [Commensurate Spin-Density Wave State in \$\(\text{TMTTF}\)_2\text{Br}\$: Single-Particle and Collective Charge Dynamics](#)
S. Tomi, N. Biskup, S. Dolanski Babi *et al.*
- [Zero-Field Muon Spin Rotation Studies in \$\(\text{TMTSE}\)_2\text{PF}_6\$](#)
L. P. Le, G. M. Luke, B. J. Sternlieb *et al.*
- [NMR and EPR Approaches to Magnetic Properties of \$\(\text{TMTTF}\)_2\text{Br}\$](#)
P. Wzietek, C. Bourbonnais, F. Creuzet *et al.*

Recent citations

- [Evidence for solitonic spin excitations from a charge-lattice-coupled ferroelectric order](#)
K. Sunami *et al*
- [From charge- and spin-ordering to superconductivity in the organic charge-transfer solids](#)
R.T. Clay and S. Mazumdar
- [Magnetic resonance investigation for a possible antiferromagnetic subphase in \$\(\text{TMTTF}\)_2\text{Br}\$](#)
Mizue Asada and Toshikazu Nakamura

NMR in Commensurate and Incommensurate Spin Density Waves.

E. BARTHEL (*), G. QUIRION (*), P. WZIETEK (*), D. JÉROME (*), J. B. CHRISTENSEN (**)
M. JØRGENSEN (**), and K. BECHGAARD (**)

(*), *Laboratoire de Physique des Solides, Associé au CNRS
UPS Bât. 510, 91405 Orsay, France*

(**), *CISMI, University of Copenhagen - Blegdamsvej 21, DK-2100, Denmark*

(received 12 August 1992; accepted in final form 16 October 1992)

PACS. 75.30F – Spin-density waves.

PACS. 76.60 – Nuclear magnetic resonance and relaxation.

PACS. 72.15N – Collective modes; low-dimensional conductors (inc. synthetic metals).

Abstract. – We present ^{13}C NMR lineshapes and spin lattice relaxation measurements of $(\text{TMTTF})_2\text{Br}$ and $(\text{TMTSF})_2\text{PF}_6$ in the spin density wave (SDW) state. We confirm that $(\text{TMTSF})_2\text{PF}_6$ has an incommensurate SDW and show that the phason mode is dominant in the relaxation. We prove that $(\text{TMTTF})_2\text{Br}$ is commensurate and estimate the SDW amplitude. No phason contribution to the relaxation is observed in this compound. The implications for theory are discussed.

Introduction. – The dynamics of spin density wave (SDW) systems has aroused much interest lately [1]. Extensive measurements on $(\text{TMTSF})_2\text{PF}_6$ (TMTSF is tetramethyl-tetraselenafulvalene) or similar compounds have pointed out distinct features, shared also by charge density waves (CDW), such as nonlinear d.c. conductivity with a marked threshold field [2], low-frequency pinned mode in a.c. conductivity [3], noise generation in the nonlinear regime [4]. This coherent set of transport properties is explained by the picture of an incommensurate SDW, *i.e.* no multiple of the wave vector of the electronic modulation is a vector of the reciprocal lattice. In this case, the collective translation mode (phason mode) is expected to have a small gap, due only to impurity pinning, and therefore dominates the dynamics of these systems.

More is needed, however, to fully understand the SDW state in quasi-one-dimensional organic conductors. In the generalised temperature-pressure phase diagram for the isostructural families $(\text{TMTTF})_2\text{X}$ (TMTTF is tetramethyltetrathiofulvalene) and $(\text{TMTSF})_2\text{X}$, with $\text{X} = \text{PF}_6, \text{SbF}_6, \text{Br}$, etc., the compounds with a SDW ground state are divided into two classes by their normal-state properties [5]. Some, like $(\text{TMTSF})_2\text{PF}_6$, are conductors down to the SDW transition, while others, like $(\text{TMTTF})_2\text{Br}$, exhibit charge localization around 100 to 200 K, and are very good insulators at the SDW transition temperature. As a result, no in-depth transport characterization of this latter class of compounds has been performed to date, and their SDW dynamics is unknown.

NMR, on the other hand, is unaffected by this charge localization, due to the one-dimensional spin-charge decoupling [6]. Moreover, it has already been extensively used

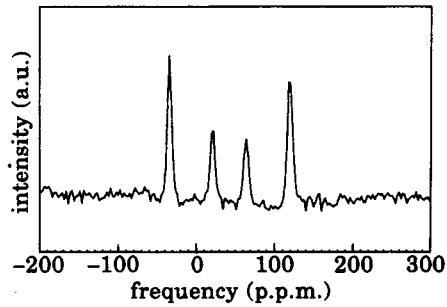


Fig. 1. - Single-crystal NMR lineshape of $(\text{TMTTF})_2\text{Br}$ at room temperature. The shift reference is TMS.

in the study of incommensurate systems like distortive crystals [7], CDW [8], and SDW [9-11], providing data on the incommensurability through lineshape analysis and on the dynamics through nuclear spin lattice relaxation (NSLR) measurements. It is therefore suitable for comparing the two classes of SDW systems.

We have measured the NMR spectrum and NSLR of both $(\text{TMTTF})_2\text{Br}$ and $(\text{TMTSF})_2\text{PF}_6$. The incommensurate nature of the SDW in $(\text{TMTSF})_2\text{PF}_6$ is confirmed. However, we show that $(\text{TMTTF})_2\text{Br}$ behaves quite differently, with a commensurate SDW. The significance of these results for the theoretical understanding of the SDW state is discussed.

Experimental. - Our samples are selectively ^{13}C -enriched on the central carbon sites usually labelled C(3) and C(13) [12] at 100% for $(\text{TMTTF})_2\text{Br}$ and at 10% per molecule for $(\text{TMTSF})_2\text{PF}_6$. The synthesis of the enriched compounds will be published shortly [13].

The $(\text{TMTSF})_2\text{PF}_6$ samples have been checked by transport measurements. The SDW transition occurs at 12.5 K. The $(\text{TMTTF})_2\text{Br}$ samples are notoriously more difficult to grow. We could not achieve good contacts for resistivity measurements, because of the poor surface quality, but the samples have been characterized by EPR. The transition occurs around 15 K.

The NMR measurements have been performed in a 9.3 T field, which brings the ^{13}C resonance frequency to 99.63 MHz. The shifts reported in fig. 1, 2 and 3 are relative to a tetramethylsilane (TMS) signal. All the data in the SDW state were obtained by an echo with phase cycling procedure. NSLR was measured by saturation recovery.

Results. - Since the four central carbon sites in the unit cell are related by inversion [12], there are only two unequivalent sites as far as NMR is concerned. Moreover, due to the

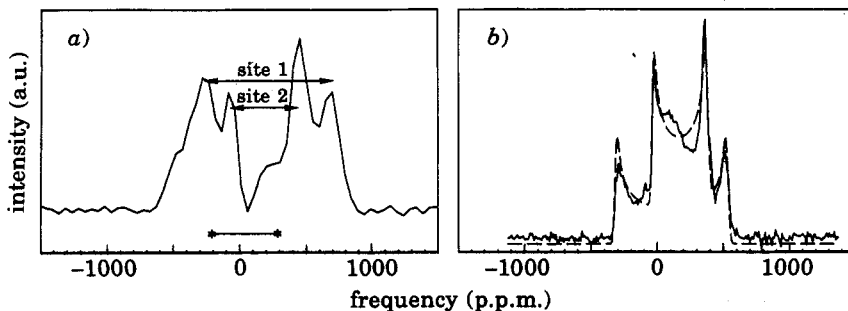


Fig. 2. - Single-crystal lineshapes in the SDW state at 4.2 K a) of $(\text{TMTTF})_2\text{Br}$ (the * — * line represents the total width of fig. 1), b) of $(\text{TMTSF})_2\text{PF}_6$. The dashed line is a fit using a sum of two functions f with different parameters ω_0 (eq. (3)). It gives equal intensity to each site.

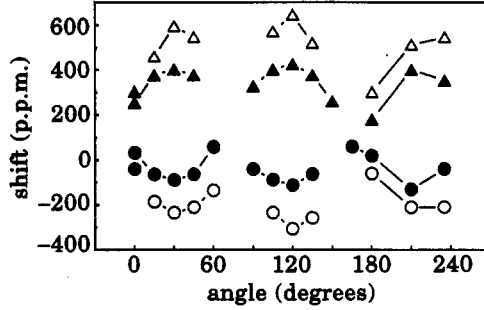


Fig. 3. - NMR shifts of the four peaks of the $(\text{TMTTF})_2\text{Br}$ lineshape in the SDW state at 12.5 K as a function of the angle of rotation around \bar{a} .

presence of intramolecular dipolar coupling, the 100% enriched $(\text{TMTTF})_2\text{Br}$ spectrum at room temperature (fig. 1) exhibits the two doublets expected for a system of two unequivocal spins dipolarly coupled. The NMR shift due to an electronic magnetization \bar{M} reads

$$S_i = \gamma/2\pi\bar{z} \cdot \bar{A}(i) \cdot \bar{M}, \quad i = 1, 2, \quad (1)$$

where γ is the gyromagnetic ratio, \bar{z} is the unit vector along the external field \bar{H}_0 and $\bar{A}(i)$ is the electron nucleus interaction tensor at site i . For comparison with the SDW state, where a staggered magnetization appears, we determined the contribution S_p (Knight shift) of the uniform electronic magnetization $\bar{M} = \chi\bar{H}_0$ to the shift in the normal phase using the large temperature dependence of the spin susceptibility χ [14]. Then, as is well known [15], the dependence of S_p upon rotation of the crystal, with different initial orientations, enables one to determine the Knight-shift tensor $\bar{K}(i) = \chi\bar{A}(i)$ for each site. Using this procedure, we find the principal axes close to \bar{a} and to the molecular symmetry axes with respective eigenvalues at room temperature given in table I.

Because of the low enrichment of our $(\text{TMTSF})_2\text{PF}_6$ samples, we were able to perform only an approximate determination of the Knight-shift tensor assuming the axes are the same as in $(\text{TMTTF})_2\text{Br}$ and using an assembly of several single crystals aligned along \bar{a} . The values we obtained are given in table II.

The total width of the lineshape of $(\text{TMTTF})_2\text{Br}$ at 4.2 K, in the SDW state (fig. 2a), is about five times larger than in the normal state. The dipolar coupling is now unresolved, and the contribution of the two sites is split up into four very different resonances, symmetrically

TABLE I. - Knight-shift anisotropy values in p.p.m. at room temperature in $(\text{TMTTF})_2\text{Br}$. The principal axes 1, 2, 3 are close, respectively, to \bar{a} , to the long molecular axis C(13)-C(3), and to the short molecular axis.

	K_1	K_2	K_3
site 1	515	- 225	- 290
site 2	385	- 170	- 215

TABLE II. - Approximate Knight-shift anisotropy values in p.p.m. at room temperature in $(\text{TMTSF})_2\text{PF}_6$. We assumed the axes are about the same as in $(\text{TMTTF})_2\text{Br}$. K_\perp is the mean value in the plane normal to \bar{a} , and ΔK_\perp is the anisotropy in this plane.

	K_a	K_\perp	ΔK_\perp
site 1	260	- 130	30
site 2	140	- 70	15

shifted with respect to the common chemical shift value. This splitting is obviously due to the presence of the staggered magnetization \bar{M}_j (the subscript j denotes that \bar{M} is no longer uniform), and to the absence of continuous distribution, we conclude that the SDW is commensurate. Since the SDW phenomenologically behaves like an antiferromagnet, the orientation of the electronic-spin magnetization is now determined by the external field and the magnetic-anisotropy tensor. In our experiments, we can rotate the single crystal around its \bar{a} axis, which is oriented perpendicular to the external field. Since the latter is much larger than the spin flop field (0.5 T), and since the hard axis is close to \bar{a} , the magnetization will stay in a direction perpendicular both to \bar{a} and to \bar{H}_0 . As a result, from eq. (1) and table I, we calculate that the shift upon rotation by θ is simply

$$S_{si,j}(\theta) = (\gamma/2\pi\chi)(K_3^{(i)} - K_2^{(i)}) \cos \theta \sin \theta M_j, \quad (2)$$

as observed (fig. 3).

However, the ratio of the relative peak positions is significantly different from the Knight-shift ratio we measured. Thus, we suppose that a slight molecular spin density redistribution occurs in the SDW state. As a result, the exact peak assignment is doubtful. One possibility, shown in fig. 2a), implies cell doubling and suggests the wave vector is $(1/2, 1/2, 0)$ or $(1/2, 0, 0)$ in the $(\bar{a}^*, \bar{b}^*, \bar{c}^*)$ basis. Another possibility is that each site contribution is split into four resonances, and that the couplingconstant difference accounts for the peak inhomogeneity we noticed through T_2 measurements. The wave vector in this case is $(1/2, 1/4, 0)$.

Despite these ambiguities, we can estimate the magnetization, using eq. (2), the data of fig. 3, the Knight shifts of table I and the room temperature spin susceptibility $\chi = 5.3 \cdot 10^{-4}$ e.m.u./mole [16]. We find that, in any case, the magnetic moment is more than $7 \cdot 10^{-2} \mu_b$ per electron and less than $1.7 \cdot 10^{-1} \mu_b$ per electron, which is consistent with the $8 \cdot 10^{-2} \mu_b$ per molecule (or $1.6 \cdot 10^{-1} \mu_b$ per electron), calculated in ref. [17].

The $(\text{TMTSF})_2\text{PF}_6$ spectrum at 4.2 K (fig. 2b)) is in sharp contrast to the previous one. It features two wide distributions of resonance frequencies, each associated with one unequivalent site. The lineshape reflects the spatial distribution of the local field at the nuclear sites. If we assume an incommensurate plane-wave modulation, this distribution is

$$f(\omega) = \begin{cases} \frac{1}{\pi} \frac{1}{\sqrt{\omega_0^2 - \omega^2}}, & \text{if } |\omega| < \omega_0, \\ 0, & \text{otherwise,} \end{cases} \quad (3)$$

where ω_0 is the distribution width related to the magnetization amplitude. Thus, our spectrum confirms the incommensurate nature of the SDW in $(\text{TMTSF})_2\text{PF}_6$. However, in our case, the lineshape is independent of the SDW wave vector. The analysis of the behaviour of the lineshape upon rotation is less straightforward in this case, because the anisotropy axes are different [17]. Relying on our approximate measurement of the shift tensor and the width of the spectrum when the easy axis \bar{b}' is normal to \bar{H}_0 , and using the room temperature susceptibility $\chi = 2.4 \cdot 10^{-4}$ e.m.u./mole [18], we tentatively estimate the magnetization amplitude to be about $6 \cdot 10^{-2} \mu_b$ per electron. Other estimates give $8 \cdot 10^{-2} \mu_b$ per molecule [9, 10] and $16 \cdot 10^{-2} \mu_b$ per molecule [17].

The temperature dependence of the NSLR of ^{13}C has also been measured in both samples. The NSLR of $(\text{TMTSF})_2\text{PF}_6$ as a function of temperature (fig. 4b)) exhibits two definite characteristics: 1) it diverges at the phase transition; 2) it remains large and constant below the critical region. Similar results have already been obtained by proton NMR [11]. The plateau in our data, obtained by ^{13}C NMR, is much clearer than in ref. [11], however, probably because the ^1H NSLR includes a strongly-temperature-dependent methyl-group

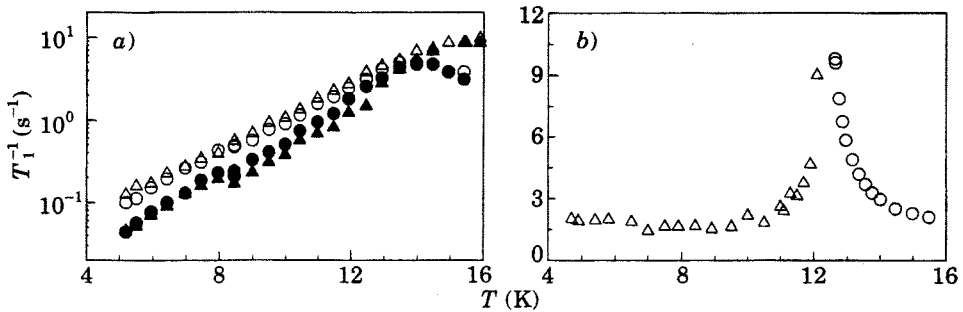


Fig. 4. – Nuclear spin lattice relaxation *a*) of $(\text{TMTTF})_2\text{Br}$ in the SDW state for the four peaks (same symbols as in fig. 3), *b*) of $(\text{TMTSF})_2\text{PF}_6$. (Δ for the SDW state, \circ for the faster peak in the normal state.)

rotation contribution. This behaviour contrasts markedly with the NSLR measured on $(\text{TMTTF})_2\text{Br}$ (fig. 4*a*)), which decreases by two orders of magnitude between the transition temperature and 4.2 K.

Great care was taken when processing the data to integrate a narrow frequency width. In the case of $(\text{TMTSF})_2\text{PF}_6$, we selected regions in which only one site contributed to the spectrum. The resulting relaxation curves, however, were strongly nonexponential in the SDW state, whereas no departure from exponentiality was observed in the normal state. Therefore, we used a stretched exponential function $M(t) = M_0(1 - \exp[-(t/T_1)^\beta])$ with an exponent $\beta = 0.65$ to fit the data in the SDW state. We analyse a stretched exponential in terms of inhomogeneity inside the sample, which induces a spatial distribution in the relaxation mode density of states and therefore a continuous distribution of T_1 's. Strong pinning in the incommensurate SDW of $(\text{TMTSF})_2\text{PF}_6$ is readily invoked to explain this inhomogeneity. In $(\text{TMTTF})_2\text{Br}$, we tentatively ascribe it to the peak inhomogeneity.

Discussion. – In the case of $(\text{TMTSF})_2\text{PF}_6$, the concept of SDW is more readily understandable: the electron-electron repulsion leads to an electronic instability. The single-electron interchain motion stabilises the ordering, which is forbidden for a strictly 1D system. Therefore, the details of the instability, like the wave vector of the modulation, are determined by the Fermi surface. Yet, for the $(\text{TMTTF})_2\text{Br}$ class of compounds, which have a gap in the electronic-charge degrees of freedom, another theory had to be developed to explain the SDW ground state [19]. It is based on a coherent interchain tunnelling of electron-hole pairs, and predicts that, despite the different mechanism, the macroscopic properties in the SDW are essentially the same in both classes of compounds: for instance, the expected SDW wave vector is also determined by the same best nesting condition of the fictitious Fermi surface [20]. In the case of $(\text{TMTSF})_2\text{PF}_6$, the NMR measurements of the SDW wave vector [9, 10] and the estimate calculated from the band structure [21] were in good agreement. In $(\text{TMTTF})_2\text{Br}$, we found that the magnetization amplitude has the expected small magnitude. Moreover, the result of the wave vector calculations at room temperature (for which transfer integral estimates are available) gives 0.37 or 0.26 for the \bar{b}^* component of the wave vector [21], which may be consistent with our observations. The origin of the commensurability (purely accidental or driven by a specific force) is thus uncertain.

As far as the NSLR is concerned, the divergence at the phase transition is known to signal the divergence of the relevant magnetic susceptibility [11]. We want to emphasize its temperature independence below the critical-temperature region. Although magnetic impurities can yield a stretched exponential relaxation shape and a NSLR independent of

temperature, we point out that the relaxation shape is very different above and below the SDW transition. Moreover, no magnetic-impurity contribution to the EPR susceptibility has been detected in our usual $(\text{TMTSF})_2\text{PF}_6$ samples. As a result, we rule out magnetic-impurity relaxation, and believe the temperature independence of the NSLR reflects the predominance of the phason mode fluctuations in the NSLR. Such a behaviour has already been observed in the incommensurate distortive crystals [7]. Therefore, the absence of this mode in the commensurate $(\text{TMTTF})_2\text{Br}$ is not surprising since commensurability is expected to introduce a significant gap, or to totally suppress the phason mode. Thus, in this latter compound, the relaxation is probably driven by magnons.

Conclusion. – We have shown that in the incommensurate SDW system $(\text{TMTSF})_2\text{PF}_6$, the phason mode dominates the NSLR. We observed that $(\text{TMTTF})_2\text{Br}$ has about the same magnetization amplitude as other SDW compounds, yet exhibits a commensurate order. As a result, the phason mode is not significant for relaxation in this compound. The wave vector may also be consistent with the theory. The NMR study of the sliding state will be the topic of a forthcoming publication.

* * *

We are grateful to J. C. AMELINE for building the probe and for help during the experiments. EB acknowledges support from the Etudes Doctorales de l'École Polytechnique. This work has been partly supported by the ESPRIT Basic Research contract MOLCOM 3121.

REFERENCES

- [1] For a review, see KRIZA G. *et al.*, *Synth. Met.*, in *Proceedings of the Conference ICSM92*, to be published or KRIZA G. *et al.*, *Europhys. Lett.*, **16** (1991) 585.
- [2] TOMIC S. *et al.*, *Synth. Met. B*, **27** (1988) 645.
- [3] QUINLIVAN D. *et al.*, *Phys. Rev. Lett.*, **65** (1990) 1816.
- [4] KRIZA G. *et al.*, *Phys. Rev. Lett.*, **66** (1991) 1922.
- [5] See, for instance, BECHGAARD K. and JÉRÔME D., *Phys. Scr.*, **T 39** (1991) 37 for a recent review.
- [6] VACA P. and COULON C., *Phase Transitions*, **30** (1991) 49.
- [7] BLINC R., *Phys. Rep.*, **79** (1981) 331.
- [8] See, for instance, BERTHIER C. *et al.*, in *Nuclear Spectroscopy on CDW Systems*, edited by T. BUTZ and A. LERF (1992).
- [9] TAKAHASHI T. *et al.*, *J. Phys. Soc. Jpn.*, **55** (1986) 1364.
- [10] DELRIEU J. M. *et al.*, *J. Phys. (Paris)*, **47** (1986) 839.
- [11] TAKAHASHI T. *et al.*, *Physica B*, **143** (1986) 417.
- [12] GALIGNÉ J. L. *et al.*, *Acta Crystallogr. B*, **34** (1978) 620; THORUP N. *et al.*, *Acta Crystallogr. B*, **37** (1981) 1236.
- [13] CHRISTENSEN J. B., JØRGENSEN M. and BECHGAARD K., to be published.
- [14] PARKIN S. S. P. *et al.*, *Phys. Rev. B*, **26** (1982) 6319.
- [15] MEHRING M., *Principles of High Resolution NMR in Solids* (Springer Verlag) 1983.
- [16] DELHAES P. *et al.*, *Mol. Cryst. Liq. Cryst.*, **50** (1979) 43.
- [17] ROGER M. *et al.*, *Phys. Rev. B*, **34** (1986) 4952.
- [18] MORTENSEN K. *et al.*, *Phys. Rev. Lett.*, **46** (1981) 1234.
- [19] BOURBONNAIS C. and CARON L. G., *Int. J. Mod. Phys. B*, **5** (1991) 1033.
- [20] CARON L. C. and BOURBONNAIS C., *J. Phys. (Paris)*, **49** (1988) C8 1419.
- [21] YAMAJI K., *J. Phys. Soc. Jpn.*, **56** (1986) 860.